



Volatile element evolution of chondrules through time

Brandon Mahan^{a,1}, Frédéric Moynier^{a,b}, Julien Siebert^{a,b}, Bleuenn Gueguen^{c,d}, Arnaud Agranier^c, Emily A. Pringle^{a,e}, Jean Bollard^f, James N. Connelly^f, and Martin Bizzarro^{a,f}

^aInstitut de Physique du Globe de Paris, Université Paris Diderot, Sorbonne Paris Cité, CNRS UMR 7154, 75238 Paris Cedex 05, France; ^bInstitut Universitaire de France, 75005 Paris, France; ^cLaboratoire Géosciences Océan, UMR CNRS 6538, Université de Bretagne Occidentale et Institut Universitaire Européen de la Mer, 29280 Plouzané, France; ^dUMS CNRS 3113, Institut Universitaire Européen de la Mer, 29280 Plouzané, France; ^eScripps Institution of Oceanography, University of California, San Diego, La Jolla CA 92093; and ^fCenter for Star and Planet Formation, University of Copenhagen, DK-1350 Copenhagen, Denmark

Edited by Mark H. Thiemens, University of California, San Diego, La Jolla, CA, and approved July 9, 2018 (received for review April 27, 2018)

Chondrites and their main components, chondrules, are our guides into the evolution of the Solar System. Investigating the history of chondrules, including their volatile element history and the prevailing conditions of their formation, has implications not only for the understanding of chondrule formation and evolution but for that of larger bodies such as the terrestrial planets. Here we have determined the bulk chemical composition—rare earth, refractory, main group, and volatile element contents—of a suite of chondrules previously dated using the Pb–Pb system. The volatile element contents of chondrules increase with time from ~1 My after Solar System formation, likely the result of mixing with a volatile-enriched component during chondrule recycling. Variations in the Mn/Na ratios signify changes in redox conditions over time, suggestive of decoupled oxygen and volatile element fugacities, and indicating a decrease in oxygen fugacity and a relative increase in the fugacities of in-fluxing volatiles with time. Within the context of terrestrial planet formation via pebble accretion, these observations corroborate the early formation of Mars under relatively oxidizing conditions and the protracted growth of Earth under more reducing conditions, and further suggest that water and volatile elements in the inner Solar System may not have arrived pairwise.

cosmochemistry | planetary formation | pebble accretion | Solar System evolution | meteorites

Primitive undifferentiated meteorites—chondrites—provide glimpses into the nascent Solar System, as their parent bodies are thought to have accreted within the first ~5 My after its formation at ~4,567 Ma, as taken from the age of Ca- and Al-rich inclusions (CAIs) (1). However, bulk chondritic meteorites are complex mélanges of materials that possibly did not form at the same time and/or under the same conditions (2), and, as such, they can provide only generic, fragmented views into the origin and evolution of Solar System solids. Furthermore, when taking both elemental and isotopic composition into account, bulk chondrite origin stories fall short of comprehensively explaining the details of Solar System evolution and terrestrial planet formation (3–8).

Chondrules on the other hand, which are the main constituents of chondrites and, like Earth, are generally depleted in moderately volatile and volatile elements (hereafter collectively termed volatile) compared with bulk chondrites (9–14), may provide more promising pathways toward terrestrial planet formation (15, 16). Pb–Pb ages indicate that most chondrules formed within 1 My after the birth of the Solar System (1, 17). Furthermore, Ca isotopes suggest that the bulk of Earth's mass, and that of the inner Solar System, accreted well within the first million years of the Solar System's existence (18). This latter study further proposes secular volatile element enrichment via the influx of outer Solar System materials, and such events are reflected in the younger, recycled chondrules which record complex heating and remelting of precursor materials over at least 4 My (17, 18). Pebble accretion of chondrule-size materials has proven a viable mechanism to reproduce the basic size and mass distribution of the Solar System on appropriate timescales (15, 16), and, furthermore, corroborates the early influx and

subsequent removal of water from the inner Solar System (19). Cumulatively, the above observations highlight chondrules as viable source materials for the majority of inner Solar System bodies, and, in this light, chondrules likely record the processes dominating inner Solar System volatile element systematics.

The behavior of elements during melting, evaporation, and condensation depends on the resident thermodynamic conditions. Exploring the compositional evolution of individual chondrules through time, especially for volatile elements that are acutely sensitive to changing conditions, can shed light on prevailing conditions during chondrule formation and recycling. For example, the Mn/Na ratio of Solar System materials is an established gauge of the prevailing oxygen fugacity conditions (fO_2) during volatilization (20, 21). This is because Mn condenses as a divalent species and Na condenses monovalently, and, as such, they express differential sensitivity to fO_2 , i.e., Mn is relatively less volatile than Na at higher fO_2 . Taken together, volatile element contents and Mn/Na ratios for individual, Pb–Pb dated chondrules remark on the prevailing history of the early inner Solar System and provide time-specific, detailed information on evolving volatile contents and redox conditions during the planet-forming epoch.

Here, we report the only elemental abundance data that currently exist for individually dated chondrules, all of which have been extracted from two of the most primitive chondrites, the L3.10 ordinary chondrite (OC), NWA 5697, and the CR2 carbonaceous chondrites, NWA 6043 (17). Element abundance data fill important informational gaps for the rare earth element

Significance

We present time-anchored elemental abundance data for some of the Solar System's first solids by tracking Pb–Pb dated chondrule compositions. Volatile element contents generally rise, while redox conditions (based on chondrule Mn/Na ratios) decline beginning ~1 My after Solar System formation (~4,567 Ma). These results reflect a continued rise in volatile element contents and their fugacities during chondrule recycling, and early water influx to the inner Solar System followed by its express removal. These observations support the early formation of Mars under oxidizing condition and Earth's protracted growth under more reducing conditions in an environment increasing in volatile contents with time, while also calling into question the coupling of water and volatile elements during Solar System evolution.

Author contributions: F.M. designed research; B.M., F.M., J.S., B.G., A.A., E.A.P., J.B., J.N.C., and M.B. analyzed data; and B.M. wrote the paper with contributions from F.M., J.S., J.N.C. and M.B.

The authors declare no conflict of interest.

This article is a PNAS Direct Submission.

This open access article is distributed under [Creative Commons Attribution-NonCommercial-NoDerivatives License 4.0 \(CC BY-NC-ND\)](https://creativecommons.org/licenses/by-nc-nd/4.0/).

¹To whom correspondence should be addressed. Email: mahan@ipgg.fr.

This article contains supporting information online at www.pnas.org/lookup/suppl/doi:10.1073/pnas.1807263115/-DCSupplemental.

Published online August 6, 2018.

(REE) patterns of L chondrite chondrules, as well as the volatile element contents of both L and CR chondrite chondrules. Volatile element abundances and Mn/Na ratios have then been investigated as a function of age to constrain the evolution of volatile contents and provide first-order insights into the prevailing redox conditions during chondrule formation for the first ~4 My of the inner Solar System. These observations, in turn, are placed within the context of Solar System evolution and terrestrial planet formation to provide time-anchored constraints on the conditions of formation for Mars and Earth, and to assess the paradigmatic view that water and volatile elements arrived in the inner Solar System contemporaneously.

Trace Element Results for Individual Chondrules

Eight chondrules from L3.10 NWA 5697 and three chondrules from CR2 NWA 6043 were analyzed for REEs, six refractory and main component elements—W, Zr, Mo, Ti, Nb, and Cr—and nine volatile elements—Mn, Ag, Sb, Na, Rb, Cs, Zn, Sn, and Cd. REEs have been conventionally listed in order of decreasing atomic radius for clarity and ease of comparison with other studies; all other elements have been reported in order of increasing volatility under solar nebula conditions (22). All element data are reported herein as La- and CI chondrite-normalized abundances (see *Materials and Methods*). Host meteorite, Pb–Pb age, and other relevant details for all chondrules can be found in Table 1 (17), along with calculated Mn/Na ratios for each chondrule. La- and CI-normalized concentrations for volatile elements are reported in Fig. 1 and Table 2, and La- and CI-normalized data for all elements are reported in *SI Appendix, Table S1* along with literature data, with La-normalized abundances in *SI Appendix, Table S2* and literature data in *SI Appendix, Table S3*.

The REE abundances for CR chondrite chondrules are in good agreement with literature values (*SI Appendix, Fig. S1 and Table S1*), validating the choice of La as a normalizing agent and, more importantly, the data set as a whole. REE abundance data for L chondrite chondrules are by-and-large novel, and, as such, there are very limited data for comparison (9); however, the few available literature values are in good agreement, and the data presented herein shed light on L chondrite chondrule composition (*SI Appendix, Fig. S1 and Table S1*). In both the L and CR chondrite chondrules, refractory and main group elements are relatively more enriched than volatile elements, especially those with 50% condensation temperatures (T_{50}) below ~800 K, consistent with the generally volatile-depleted nature of chondrules relative to bulk meteorites (13) (Fig. 1).

Table 1. Host meteorite, Pb–Pb age and information for individual chondrules

| Chondrule | Pb–Pb age | Type | Ol. Fa# | Mn/Na |
|------------------|-----------------|------|---------|-------|
| NWA 5697 (L3.10) | | | | |
| 2-C1 | 4,567.57 ± 0.56 | I | 6.1 | 0.5 |
| 5-C2 | 4,567.54 ± 0.52 | II | 19 | 2.2 |
| 5-C10 | 4,567.41 ± 0.57 | II | 19 | 2.7 |
| D-C3 | 4,566.58 ± 0.57 | II | 27 | 3.3 |
| 5-C4 | 4,566.56 ± 0.53 | II | 12 | 2.9 |
| 3-C5 | 4,566.20 ± 0.63 | II | 19 | 2.5 |
| 11-C2 | 4,564.65 ± 0.46 | II | 22 | 0.8 |
| 3-C2 | 4,563.64 ± 0.51 | II | 15 | 1.2 |
| NWA 6043 (CR2) | | | | |
| 1-C2 | 4,567.26 ± 0.37 | I | 9.8 | 1.5 |
| 2-C2 | 4,565.06 ± 0.40 | II | 23.9 | 1.9 |
| 2-C4 | 4,563.64 ± 0.51 | II | 13.5 | 1.5 |

Pb–Pb ages, chondrule type, and olivine fayalite number (Ol. Fa#) from ref. 17. Manganese-to-sodium ratios (Mn/Na) are from the current study.

The majority of data are for chondrules from L3.10 NWA 5697, providing a more complete picture of L chondrite chondrule evolution. Therefore, discussion focuses largely on these chondrules, and, where possible, complementary observations are presented for the chondrules of the CR2 chondrite NWA 6043.

Comparison with Other Chondrules, Bulk Chondrites, and the Bulk Earth

REE patterns for both L and CR (to a lesser degree) chondrite chondrules are similar to that of their host meteorites (*SI Appendix, Fig. S1*), indicating that the REE contents of chondrules largely set the budget of these elements in the bulk. This is likely owing to chondrules constituting over half the bulk or more by volume in both cases (>60% for OCs) (23, 24). Bulk chondritic patterns are more closely mirrored by older chondrules in CR chondrite chondrules for refractory and main group elements (Fig. 1). For L chondrite chondrules, La- and CI-normalized data indicate that refractory and main group elements are similar to bulk L chondrites and chondrules (where data exist) (Fig. 1). For both L and CR chondrite chondrules, these observations suggest that chondrules generally control bulk chondrite element systematics, as has been previously suggested (25).

Volatile element contents for L chondrite chondrules from the current study generally fall in line with the so-called volatility trend (e.g., Na, Rb, and Cs), while bulk L chondrite values for these elements display enrichments relative to this trend, suggesting an enriched component for these elements in the host meteorite. The general volatile depletion pattern of the L chondrite chondrules is in good agreement with that for the bulk Earth (Fig. 1). Data for CR chondrules in the current work, as well as in the literature, display relatively higher variations, making further discussion largely untenable.

Age-Dependent Element Systematics

The current study provides compositional data for chondrules that are anchored in time. The abundances of Ag and Sb, and, to a lesser degree, Zn, display stochastic variations concomitant with CAI formation at ~4,567 Ma (1), followed by a general depletion and subsequent increase in abundance (Fig. 2 and Table 2). Fig. 2 reports the abundances of Ag and Sb as a function of chondrule age, as these elements display the most coherent positive trend with time, while elements of higher volatility show more variability. These data provide observational evidence for a general increase in volatile contents in the inner Solar System through time. This volatile element evolution pathway for the inner Solar System is supported by a wealth of literature across a broad range of methodological approaches, e.g., experimental petrology (26), isotope geochemistry (18, 27), and astrophysicochemical modeling (19, 28, 29). These lines of evidence, along with the likely early formation of most chondrules and their later recycling in a volatile-enhanced environment (17, 18), support the view that a fraction of the chondrule population in OCs were formed (recycled) under noncanonical conditions marked by increased volatile contents (30), and, moreover, provide time constraints for the generation of such chondrule populations. The agreement between chondrule volatile element contents and that of the bulk Earth (Fig. 1 and Table 2) further evidence a robust compositional relationship between the two, strengthening the argument that chondrule accretion played an integral role in terrestrial planet formation. More broadly speaking, the current data suggest that increased volatile flux to the inner Solar System began ~1 My after CAI formation and proceeded for at least the next 3 My (Fig. 2 and Table 2), corroborating and elaborating upon previous observations for these same chondrules (18).

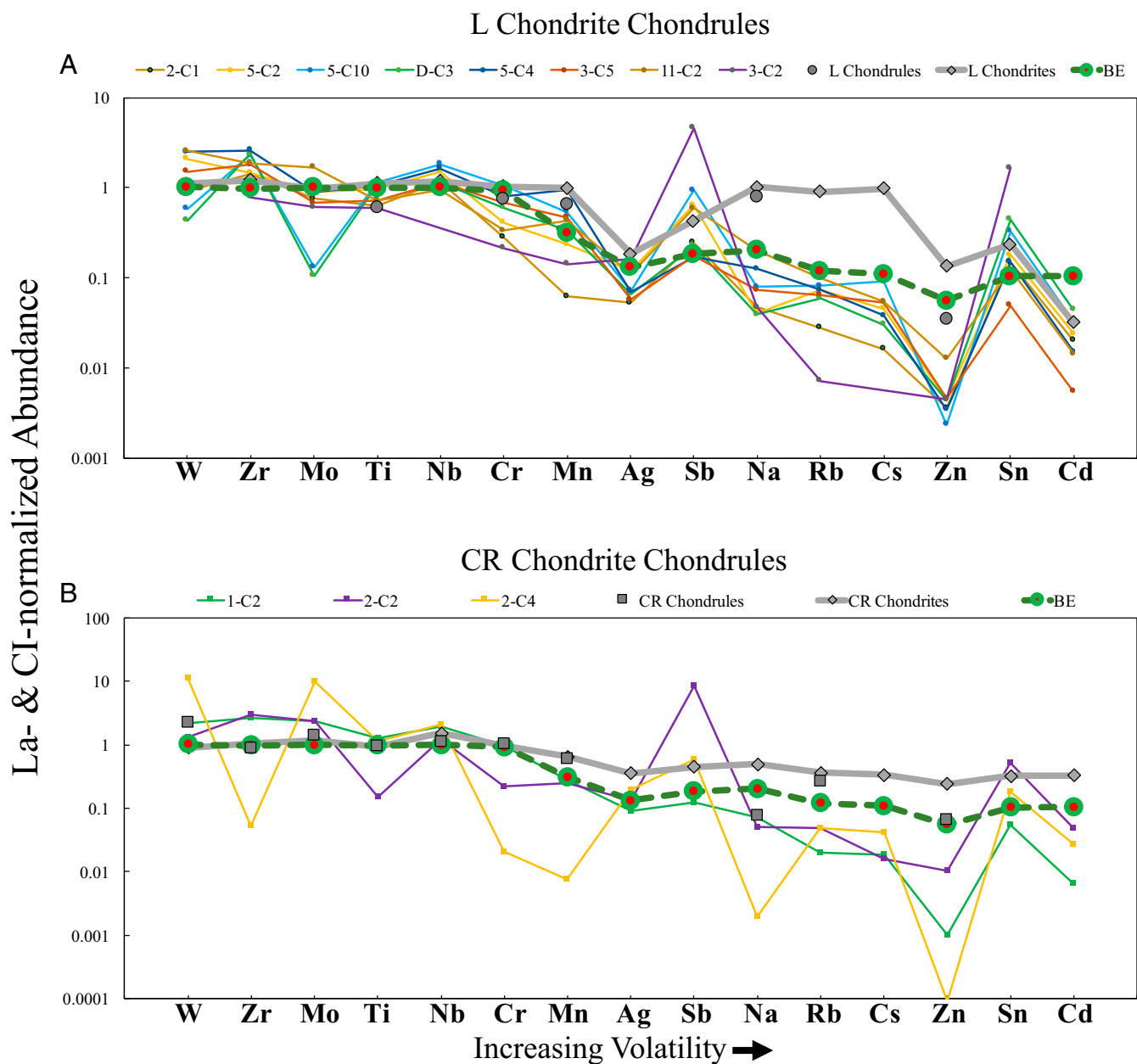


Fig. 1. La- and Cl-normalized abundances for refractory, main group, and volatile elements for (A) L and (B) CR chondrite chondrules. Where available, literature data have been included for both L and CR chondrite chondrules and their bulk meteorite hosts. Bulk Earth estimates have been averaged from refs. 40 and 42. All data are as indicated in the legend.

Manganese-to-Sodium Ratios of Individual Chondrules

The Mn/Na ratios of the L chondrite chondrules increase from ~0.5 to over 3 within approximately the first 1 My of the Solar System, and then decline to nearly the starting value (final Mn/Na ≈ 1) over the next 3 My (Fig. 3). Chondrule olivine fayalite contents (17) for L chondrite chondrules increase concomitant with Mn/Na ratios up to their highest values, further validating Mn/Na as an appropriate first-order gauge of prevailing fO_2 conditions. These results indicate an increase in fO_2 —or at least variable fO_2 —beginning with the formation of CAIs and peaking at ~4,566.5 Ma, followed by a return to more reducing conditions by ~4,564.5 Ma. This redox path is seemingly at odds with the general enrichment of volatile elements observed (Fig. 2 and Table 2), indicating coeval forces.

Reconciling Volatile Element and Mn/Na Ratio Systematics

The overall redox state of a gas–melt system and the subsequent (re)distribution of volatile elements is not only governed by oxygen fugacity but also by the fugacities of other influential elements that may be present in the gas phase, and it is likely that such mechanisms are at play here. There is ample evidence to indicate that high partial pressures of volatile elements (e.g., K, Na, and S) are behind the simultaneously reduced and volatile-enriched nature of OCs and their chondrules (30, 31). A volatile-rich but water-poor (dry) environment after ~1 My is consistent with the observed general increase in volatile element contents in the younger chondrules and the subsidence of more oxidizing conditions. Dry volatile influx beginning at ~4,566.5 Ma readily explains the enhanced volatile contents of L chondrite chondrules relative to CR chondrite chondrules (Table 2),

Table 2. La- and Cl-normalized volatile element abundances for individual chondrules

| Element | NWA 5697 (L3.10) | | | | | | | | NWA 6043 (CR2) | | |
|---------|------------------|-------|-------|-------|-------|-------|-------|-------|----------------|-------|-------|
| | 2-C1 | 5-C2 | 5-C10 | D-C3 | 5-C4 | 3-C5 | 11-C2 | 3-C2 | 1-C2 | 2-C2 | 2-C4 |
| Mn | 0.06 | 0.23 | 0.54 | 0.34 | 0.95 | 0.47 | 0.43 | 0.14 | 0.29 | 0.25 | 0.01 |
| Ag | 0.05 | 0.12 | 0.07 | 0.07 | 0.07 | 0.06 | 0.11 | 0.16 | 0.09 | 0.14 | 0.20 |
| Sb | 0.25 | 0.64 | 0.94 | 0.23 | 0.17 | 0.18 | 0.59 | 4.59 | 0.13 | 8.39 | 0.58 |
| Na | 0.05 | 0.04 | 0.08 | 0.04 | 0.13 | 0.07 | 0.20 | 0.05 | 0.07 | 0.05 | 0.002 |
| Rb | 0.03 | 0.07 | 0.08 | 0.06 | 0.07 | 0.06 | 0.10 | 0.01 | 0.02 | 0.05 | 0.05 |
| Cs | 0.02 | 0.05 | 0.09 | 0.03 | 0.04 | 0.05 | 0.05 | 0.00 | 0.02 | 0.02 | 0.04 |
| Zn | 0.004 | 0.004 | 0.002 | 0.004 | 0.003 | 0.005 | 0.013 | 0.004 | 0.001 | 0.010 | 0.000 |
| Sn | 0.15 | 0.18 | 0.33 | 0.44 | 0.15 | 0.05 | 0.12 | 1.66 | 0.05 | 0.51 | 0.18 |
| Cd | 0.02 | 0.02 | 0.03 | 0.04 | 0.02 | 0.01 | 0.01 | 0.00 | 0.01 | 0.05 | 0.03 |

Elements ordered from least to most volatile under solar nebula conditions (22). Please see *SI Appendix* for La- and Cl-normalized abundances for all elements (*SI Appendix, Table S1*); La-normalized values and calculated Mn/Na ratios (*SI Appendix, Table S2*); and Cl abundances used for normalization, along with literature data for the bulk Earth, L, and CR chondrites and their chondrules (*SI Appendix, Table S3*).

and explains the same observation for their bulk chondrite hosts, as well as the generally water-poor nature of OCs (and enstatite chondrites) relative to carbonaceous ones (5, 13, 23, 32). Moreover, the timing of the volatile element and redox pathway herein is fully consistent with that suggested by

astrophysicochemical models, wherein water levels in the inner Solar System increase dramatically within the first ~200 Ky (and thus fO_2), followed by decline to dry conditions after about 1 My, leading to a relative increase in the fugacities of other volatile species (19, 33). Furthermore, these results indicate a decoupling

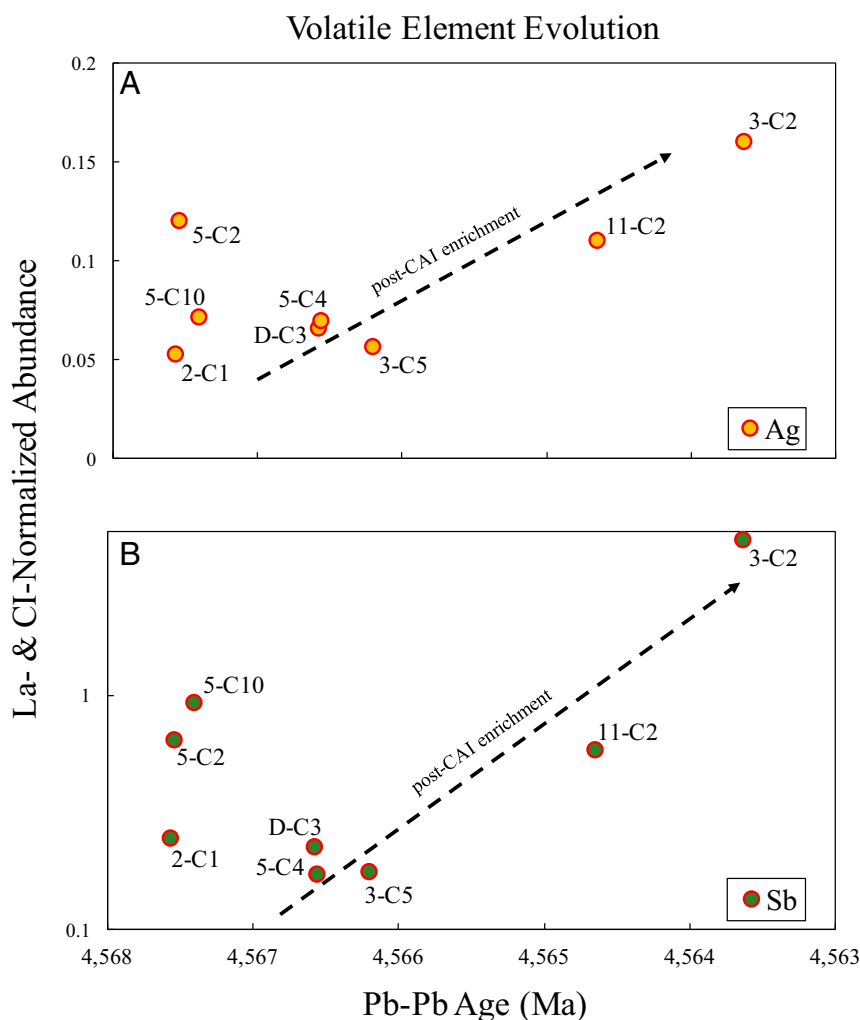


Fig. 2. La- and Cl-normalized (A) Ag and (B) Sb contents for L chondrite chondrules as a function of Pb–Pb age (17). General volatile enrichment through time indicates interaction of chondrules with a gas phase that is increasingly volatile-rich during recycling. Note the logarithmic scale for Sb in B.

L Chondrite Chondrule Redox Evolution

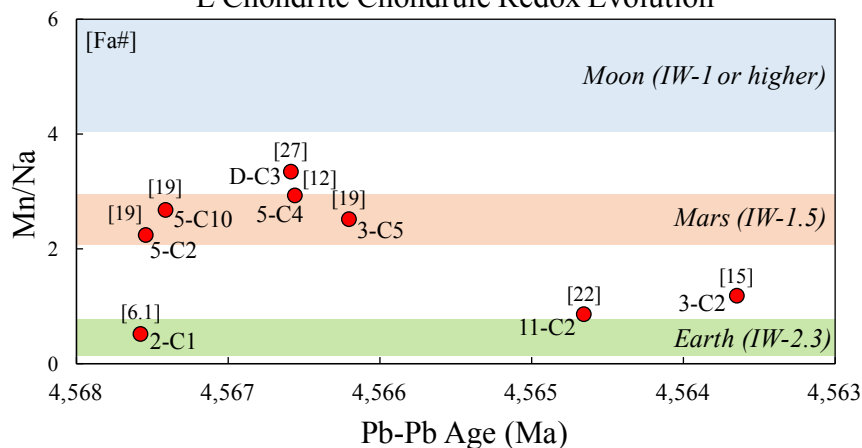


Fig. 3. Calculated Mn/Na ratios for L chondrite chondrules as a function of Pb–Pb age, with individual olivine fayalite number, Fa#, reported in brackets next to individual chondrules (17). Olivine chondrule Fa# is strongly correlated to Mn/Na for the first 1 My of the Solar System ($R^2 = 0.97$), corroborating an increase in oxygen fugacity during this time. After $\sim 4,566.5$ Ma, Mn/Na and Fa# decouple ($R^2 = 0.29$), likely due to incomplete melting of chondrules, gas interaction, and/or variable Fe retention. Typical error for Pb–Pb dating is approximately ± 0.50 My, i.e., less than the time spanned here, further validating the observed trends for Mn/Na and Fa#. For reference, Mn/Na ratios for Earth, Mars, and the Moon are reported as green, red, and blue shaded regions, respectively, along with present-day bulk fO_2 estimates (20, 26, 43, 44).

of water and volatile element evolution in the early inner Solar System, calling for a reexamination of the established notion that water and volatile elements arrived in lockstep to the inner Solar System (34).

On the Formation of Larger Solar System Bodies

Vesta and the angrite parent body are thought to have formed no later than 0.4 My after CAIs (35, 36), and the angrite parent body has the highest reported Mn/Na ratio (~ 12) of any Solar System body (20), coincident with the timing of high Mn/Na ratios determined in the current study (Fig. 3). Mars, at least half of which is thought to have accreted within the first 2 My of the Solar System (37), has an estimated Mn/Na ratio of 2 to 3 (20), a range strikingly similar to OC chondrules of the same age within the current study, suggesting that a major fraction of Mars could have accreted from OC chondrules (or at least OC-like) resident during this time and thus under similarly oxidizing conditions and increasing volatile contents (Figs. 2 and 3). Proto-Earth is thought to have experienced protracted growth up to ~ 5 My after CAIs, with $\sim 40\%$ of its accreting material potentially coming from volatile-enriched outer Solar System reservoirs (18). This growth history for Earth suggests significant accretion from a reservoir of relatively reduced chondrules, with subsequent volatile content augmentation through time via remelting/recycling in an increasingly volatile-rich environment (Figs. 2 and 3). Moreover, the volatile element and redox pathway determined in the current study indicate a need to explore the possible decoupling of water and other volatiles in petrochemical models of terrestrial planet formation and differentiation. Finally, it is possible that bodies accreting outward of Earth's orbit may have acted as volatile element sinks, based on the relatively elevated moderately volatile element contents of ordinary and enstatite chondrites and their chondrules (13, 38), the high volatile contents (e.g., S) estimated for bulk Mars (38, 39), the formation of these bodies outward of the orbit of Earth (8, 38), and the lack of such enrichments for Earth and that presumed for Venus and Mercury (5, 38, 40).

Conclusions

The compositional evolution of some of the Solar System's first solids, chondrules, has been mapped out as a function of time. These results display a general increase in chondrule volatile

contents with age, likely due to chondrule recycling under changing conditions that became more enriched in volatile elements over time. Redox conditions evolved over time, and this is recorded in chondrule Mn/Na ratios. Oxygen fugacity generally increased with time up to $\sim 4,566.5$ Ga, concomitant with volatile enrichments, and afterward displayed a more protracted decline, while volatile contents continued to rise. These observations suggest that this time ($\sim 4,566.5$ Ma) marks the onset of inner Solar System dry-out and the subsequent rise in fugacities of other volatiles such as K, Na, and S. These results provide time-anchored evidence for the early formation of proto-Mars from relatively oxidized materials, and evidence that proto-Earth formed via accretion of variably oxidized, volatile-poor chondrules, followed by appreciable addition of recycled, volatile-enhanced material under more reducing conditions. Such an accretion pathway for Earth elicits the need for formation and differentiation models which consider the decoupling of volatile element and water (redox) evolution. Lastly, the timing of formation, relative distance from the Sun, and chemical composition of Mars and the ordinary (and enstatite) chondrites indicate that perhaps these bodies incorporated the bulk of incoming volatile-rich material from cooler outer regions of the Solar System, depriving Earth and other bodies accreting inside its orbit of their full complement of volatile elements.

Materials and Methods

Dilute sample aliquots were analyzed using the high-resolution inductively coupled plasma mass spectrometer Thermo Scientific Element XR at Laboratoire Géosciences Océan (Université de Brest) for the following isotopes: ^{139}La , ^{140}Ce , ^{141}Pr , ^{146}Nd , ^{147}Sm , ^{151}Eu , ^{157}Gd , ^{159}Tb , ^{163}Dy , ^{165}Ho , ^{167}Er , ^{169}Tm , ^{174}Yb , ^{175}Lu , ^{184}W , ^{91}Zr , ^{98}Mo , ^{47}Ti , ^{93}Nb , ^{53}Cr , ^{55}Mn , ^{107}Ag , ^{121}Sb , ^{23}Na , ^{85}Rb , ^{133}Cs , ^{66}Zn , ^{118}Sn , and ^{114}Cd . All elements were calibrated using standard solutions (10, 50, 100, and 1,000 ppt), and their count rates were blank-corrected. Indium (^{115}In) was used as an internal standard to correct all data for instrumental mass bias during the analyses. Instrument precision (reproducibility) for all elements was better than 4% (1 relative SD). All analyses within the current study were performed on the same sample dissolutions from which aliquots had previously been taken for Pb–Pb dating and Zn isotopic measurements (17), rendering calculations of absolute element concentrations untenable. Therefore, all data have been normalized to La and to CI chondrites. La was chosen as an ideal normalizing element, as its concentrations in both L and CR chondrite chondrules have been previously established and anchor the results (9, 12). Furthermore, La is a

relatively refractory ($T_{50} \approx 1,580$ K) (22) and fluid-immobile element and thus is not redistributed during secondary alteration processes (41), and it is sufficiently abundant in all samples for precise measurement.

ACKNOWLEDGMENTS. We thank two anonymous reviewers for their insightful comments and constructive criticism that greatly improved the quality of this paper. We thank Sébastien Charnoz, Francesco Pignatale, Paolo Sossi, and the rest of the Cosmochimie, Astrophysique, et Géophysique Expérimentale (CAGE) team at Institut de Physique du Globe de Paris (IPGP) for fruitful discussions. We acknowledge the financial support of the Uni-Earth5 Labex program at Sorbonne Paris Cité (through French National

Research Agency (ANR) Grants ANR-10-LABX-0023 and ANR-11-IDEX-0005-02). B.M. acknowledges the financial support of the Initiative d'Excellence (IDEX), Université Sorbonne Paris Cité (USPC) through a PhD fellowship. J.S. acknowledges the financial support of the ANR (ANR Project VolTerre, Grant ANR-14-CE33-0017-01). F.M. acknowledges funding from the European Research Council (ERC) under the H2020 framework program/ERC Grant Agreement 637503 (Pristine). M.B. acknowledges funding from the Danish National Research Foundation (Grant DNRF97) and the ERC (ERC Consolidator Grant Agreement 616027, STARDUST2ASTEROIDS). Parts of this work were supported by the IPGP multidisciplinary program Plateau d'Analyse Haute Résolution (PARI), and by the Region Île-de-France SESAME Grant 12015908.

1. Connelly JN, et al. (2012) The absolute chronology and thermal processing of solids in the solar protoplanetary disk. *Science* 338:651–655.
2. Bizzarro M, Connelly JN, Krot AN (2017) Chondrules: Ubiquitous chondritic solids tracking the evolution of the solar protoplanetary disk. *Formation, Evolution, and Dynamics of Young Solar Systems*, Astrophysics and Space Science Library (Springer, New York), Vol 445, pp 161–195.
3. Burkhardt C, et al. (2011) Molybdenum isotope anomalies in meteorites: Constraints on solar nebula evolution and origin of the Earth. *Earth Planet Sci Lett* 312:390–400.
4. Warren PH (2011) Stable-isotopic anomalies and the accretionary assemblage of the Earth and Mars: A subordinate role for carbonaceous chondrites. *Earth Planet Sci Lett* 311:93–100.
5. Palme H, O'Neill HSC (2014) Cosmochemical estimates of mantle composition. *Treatise on Geochemistry* (Elsevier, New York), 2nd Ed, pp 1–39.
6. Burkhardt C, et al. (2017) In search of the Earth-forming reservoir: Mineralogical, chemical, and isotopic characterizations of the ungrouped achondrite NWA 5363/NWA 5400 and selected chondrites. *Meteorit Planet Sci* 52:807–826.
7. Dauphas N (2017) The isotopic nature of the Earth's accreting material through time. *Nature* 541:521–524.
8. Render J, Fischer-Gödde M, Burkhardt C, Kleine T (2017) The cosmic molybdenum-neodymium isotope correlation and the building material of the Earth. *Geochem Perspect Lett* 3:170–178.
9. Gooding JL, et al. (1980) Oxygen isotopic compositions of petrologically characterized chondrules from unequilibrated chondrites. *Meteoritics* 15:295.
10. Lux G, Keil K, Taylor GJ (1981) Chondrules in H3 chondrites: Textures, compositions and origins. *Geochim Cosmochim Acta* 45:675–685.
11. Hewins RH, Herzberg CT (1996) Nebular turbulence, chondrule formation, and the composition of Earth. *Earth Planet Sci Lett* 144:1–7.
12. Gerber M (2012) Chondrule formation in the early solar system: A combined ICP-MS, ICP-OES and petrologic study. PhD thesis (University of Münster, Münster, Germany).
13. Hezel DC, Harak M, Libourel G (2018) What we know about elemental bulk chondrule and matrix compositions: Presenting the ChondriteDB database. *Chem Erde* 78:1–14.
14. Amsellem E, Moynier F, Pringle EA, Day J (2017) Testing the chondrule-rich accretion model for planetary embryos using calcium isotopes. *Earth Planet Sci Lett* 469:75–83.
15. Johansen A, Low M-MM, Lacerda P, Bizzarro M (2015) Growth of asteroids, planetary embryos, and Kuiper belt objects by chondrule accretion. *Sci Adv* 1:e1500109.
16. Levison HF, Kretke KA, Walsh KJ, Bottke WF (2015) Growing the terrestrial planets from the gradual accumulation of submeter-sized objects. *Proc Natl Acad Sci USA* 112: 14180–14185.
17. Bollard J, et al. (2017) Early formation of planetary building blocks inferred from Pb isotopic ages of chondrules. *Sci Adv* 3:e1700407.
18. Schiller M, Bizzarro M, Fernandes VA (2018) Isotopic evolution of the protoplanetary disk and the building blocks of Earth and the Moon. *Nature* 555:507–510.
19. Ciesla F, Cuzzi J (2006) The evolution of the water distribution in a viscous protoplanetary disk. *Icarus* 181:178–204.
20. O'Neill HS, Palme H (2008) Collisional erosion and the non-chondritic composition of the terrestrial planets. *Philos Trans A Math Phys Eng Sci* 366:4205–4238.
21. Siebert J, et al. (2018) Chondritic Mn/Na ratio and limited post-nebular volatile loss of the Earth. *Earth Planet Sci Lett* 485:130–139.
22. Lodders K (2003) Solar system abundances and condensation temperatures of the elements. *Astrophys J* 591:1220–1247.
23. Righter K, Drake MJ, Scott ERD (2006) Compositional relationships between meteorites and terrestrial planets. *Meteorites and the Early Solar System II*, eds Lauretta DS, McSween HY (University of Arizona Press, Tucson, Arizona), pp 803–828.
24. Zanda B, Hewins RH, Bourrot-Denise M, Bland PA, Albarède F (2006) Formation of solar system nebula reservoirs by mixing chondritic components. *Earth Planet Sci Lett* 248:650–660.
25. Alexander CMOD (2005) Re-examining the role of chondrules in producing the elemental fractionations in chondrites. *Meteorit Planet Sci* 7:943–965.
26. Siebert J, Corgne A, Ryerson FJ (2011) Systematics of metal-silicate partitioning for many siderophile elements applied to Earth's core formation. *Geochim Cosmochim Acta* 75:1451–1489.
27. Schönbächler M, Carlson RW, Horan MF, Mock TD, Hauri EH (2010) Heterogeneous accretion and the moderately volatile element budget of Earth. *Science* 328:884–887.
28. Rubie DC, et al. (2015) Accretion and differentiation of the terrestrial planets with implications for the compositions of early-formed solar system bodies and accretion of water. *Icarus* 248:89–108.
29. Rubie DC, et al. (2016) Highly siderophile elements were stripped from Earth's mantle by iron sulfide segregation. *Science* 353:1141–1144.
30. Hewins RH, Zanda B (2012) Chondrules: Precursors and interactions with the nebular gas. *Meteorit Planet Sci* 47:1120–1138.
31. Hewins RH, Zanda B, Bendersky C (2012) Evaporation and recondensation of sodium in Semarkona type II chondrules. *Geochim Cosmochim Acta* 78:1–17.
32. Jacquet E, Paulhiac-Pison M, Alard O, Kearsley AT, Gounelle M (2013) Trace element geochemistry of CR chondrite metal. *Meteorit Planet Sci* 48:1981–1999.
33. Pasek M, et al. (2005) Sulfur chemistry with time-varying oxygen abundance during solar system formation. *Icarus* 175:1–14.
34. Albarède F (2009) Volatile accretion history of the terrestrial planets and dynamic implications. *Nature* 461:1227–1233.
35. Schiller M, et al. (2011) Rapid timescales for magma ocean crystallization on the howardite-eucrite-diogenite parent body. *Astrophys J Lett* 740:1–6.
36. Schiller M, Connelly JN, Glad AC, Mikouchi T, Bizzarro M (2015) Early accretion of protoplanets inferred from a reduced inner solar system ^{26}Al inventory. *Earth Planet Sci Lett* 420:45–54.
37. Dauphas N, Pourmand A (2011) Hf-W-Th evidence for rapid growth of Mars and its status as a planetary embryo. *Nature* 473:489–492.
38. Lodders K, Fegley BJ (1998) *The Planetary Scientist's Companion* (Oxford Univ Press, New York).
39. Stewart AJ, Schmidt MW, van Westrenen W, Lieske C (2007) Mars: A new core-crystallization regime. *Science* 316:1323–1325.
40. McDonough WF (2003) Compositional model for the Earth's core. *Treatise on Geochemistry*, ed Carlson RW (Elsevier, New York), Vol 2, pp 547–568.
41. Plank T (2005) Constraints from Thorium/Lanthanum on sediment recycling at subduction zones and the evolution of the continents. *J Petrol* 46:921–944.
42. Allègre C, Manhès G, Lewin É (2001) Chemical composition of the Earth and volatility control on planetary genetics. *Earth Planet Sci Lett* 185:49–69.
43. Righter K, Yang H, Costin G, Downs RT (2008) Oxygen fugacity in the Martian mantle controlled by carbon: New constraints from the nakhlite MIL 03346. *Meteorit Planet Sci* 43:1709–1723.
44. Wadhwa M (2008) Redox conditions on small bodies, the Moon and Mars. *Rev Mineral Geochem* 68:493–510.